View Article Online
DOI: 10.1039/C7TB01900A

Journal Name

ARTICLE

A Two-Photon ratiometric Fluorescent Probe for the Synergistic Detection of Mitochondrial SO_2/HClO Crosstalk in Cells and in Vivo

Received 00th January 20xx,
Accepted 00th January 20xx

DOI: 10.1039/x0xx00000x

www.rsc.org/

Kun Dou,[a,b] Guang Chen,[a,b] Fabiao Yu,[a,b]* Zhiwei Sun,[a] Guoliang Li,[a] Xianen Zhao,[a] Lingxin Chen,[a,b]*and Jinmao You[a,b]*

Known as a new member of reactive sulphur species (RSS), endogenous sulfur dioxide (SO_2) plays potential reductive roles in antioxidant, anti-aging, anti-inflammatory and cytoprotection. However, SO_2 is also a metabolite of antioxidant. Hypochlorous acid (HClO) has powerful bioeffects on the innate immune system, its uncontrolled production leads to adverse damages in cells. In order to illuminate the potential crosstalk between SO_2 and HClO in redox homeostasis, we design a two-photon ratiometric fluorescent probe for dual-response to mitochondrial SO_2/HClO crosstalk in cells and *in vivo*. Our probe can effectively achieve fluorescence ratio dual-response to SO_2 and HClO with desirable properties, such as large two-photon absorption cross sections, rapid response times (SO_2 < 50 s, HClO < 20 s), high sensitivities (limit of detection 8.0 nM for SO_2 and 15.2 nM for HClO), and favorable selectivity. The probe has been successfully applied to quantitatively detect endogenous SO_2 and HClO in HeLa and Raw 264.7 cells. We verify that there exists a crosstalk between SO_2 and HClO during the process of oxidative stress in mitochondria. We also detect SO_2 can be endogenously produced through oxidation of intracellular sulfur-containing amino acids by HClO in zebrafish in real-time.

Introduction

Reactive sulphur species (RSS) and reactive oxygen species (ROS) play critical roles in a series of physiological and pathological processes, which involve in cell proliferation, redox homeostasis regulation, neurodegenerative injury and cytoprotection.[1,2] Sulfur dioxide (SO_2) which has long been recognized as a toxic environmental pollutant is now considered to be one of the new potential gaseous signaling molecules, anti-oxidant and anti-oxidative metabolite.[3] Usually, SO_2 can be endogenously enzymatically produced in mitochondria by the oxidation of hydrogen sulfide and some sulphur-containing amino acids.[4] However, the abnormal level of SO_2 can induce lung cancer, cardiovascular diseases as well as neurological disorders.[5] Accumulated evidences imply that endogenous SO_2 plays crucial roles in mediate a wide range of physiological processes, including signal transduction, regulation of cardiovascular function, increasing anti-oxidative capacity, and regulating the intracellular redox status.[6-8] Since the intracellular oxidative stress is associated with the disorder between ROS and cellular antioxidant systems, such as RSS, the overproduction of ROS will break cellular defense systems and damage organelles.[9,10] Hypochlorous acid (HClO) is one of the important reactive oxygen species (ROS) in cells, which is endogenously produced from hydrogen peroxide and chloride ions catalyzed by the heme-enzyme myeloperoxidase (MPO).[11,12] HClO play key roles in immune defense, cell signaling, and redox homeostasis.[13] But the excessive generation of HClO will consume antioxidants and result in the imbalance of intracellular redox milieu, then cause serious mitochondrial permeabilization. As known, Alzheimer's disease, Parkinson's disease and other neurodegenerative diseases have closely relationship with protein oxidative damage that caused by the imbalance between RSS and ROS.[14,15] As the two important members of ROS/RSS, endogenous sulfur dioxide (SO_2) and hypochlorous acid (HClO) exhibit intimate relationship in maintaining redox homeostasis, regulating cardiovascular diseases, and controlling neurological disorders.[16] Although the physiological functions and the pathogenic mechanisms of SO_2 and HClO have been elegantly discussed, the biological related-effects of the two small molecules still remain largely unknown. Therefore, in view of the important roles of SO_2 and HClO in the complex signal transduction and oxidation pathways, the direct detection and illumination of crosstalk between endogenous SO_2 and HClO at the cellular level have become one of important topics in the field of biology and medicine. We strive to develop a sensitive method for the real-time monitor and effectively discriminate SO_2/HClO in cells.

Mitochondria is considered to be the main sources of intracellular ROS and is abundant in RSS where a vital organelle provides energy for the body. It is crucial to investigate how the crosstalk between SO_2 and HClO effects on mitochondria.[17-19] On account of rapid

[a] *Key Laboratory of Life-Organic Analysis, Key Laboratory of Pharmaceutical Intermediates and Analysis of Natural Medicine, College of Chemistry and Chemical Engineering, Qufu Normal University, Qufu 273165, China.*
[b] *Key Laboratory of Coastal Environmental Processes and Ecological Remediation; Research Centre for Coastal Environmental Engineering and Technology, Yantai Institute of Coastal Zone Research, Chinese Academy of Sciences, Yantai 264003, China.*
**Email - lxchen@yic.ac.cn*
Electronic Supplementary Information (ESI) available: [details of supplementary information for this work]. See DOI: 10.1039/x0xx00000x

View Article Online
DOI: 10.1039/C7TB01900A

metabolic mechanism and complicated matrix interference to intracellular redox-pair, achieving immediately recognition and determination of endogenous SO_2 and HClO with direct chemical tools is highly sought after. Many efforts had been focused on the investigations of the bioeffects of ROS and RSS.[20,21] The approaches include chromatography,[22] electrochemistry,[23] capillary electrophoresis and flow injection analysis.[24] However, considering the short lifetime and the rapid catabolism properties of SO_2 and HClO in mitochondria, a high performance method should be applied to indicate the redox process.

Compared to other bio-detection technologies, fluorescent bio-imaging technology features beneficial advantages in detecting biomolecules including non-invasion, high spatial and temporal resolution, more convenience, as well as real-time imaging. Now, many efforts have done on developing fluorescent probe for the detection of SO_2/HClO, respectively.[25-29] However, most of these probes employ single emission intensity for imaging and detection.[30,31] The major concern of the single intensity detection is that fluorescence collection may be potentially influenced by many factors, such as the instrument efficiency, uneven loading or the inhomogeneous distribution of fluorescent probes, environmental conditions, and photo-bleaching.[32] It is noteworthy that ratiometric probes which employ the ratio of the emission intensities at two different wavelengths can eliminate most the interference and can reconstruct ratiometric images for the region of interest by pixel-to-pixel. Although ratiometric fluorescence probes exhibit distinct advantages in accuracy and reliability, we have to avoid some of the limitations such as slow response time, sensitivity, and selectivity.[33,34] In terms of the sufficient penetration into tissues and the elimination of auto-fluorescence from cells, ratiometric probes which can work at longer excitation wavelengths is always expected. Two-photon (TP) probes will meet the requirements and have emerged as indispensable imaging tools for the detection of biomolecules, because two near-infrared (NIR) photons are employed as the excitation source.[35-39] Moreover, those probes which only respond to single active species are unable to clearly demonstrate the redox homeostasis process between SO_2 and HClO. We suggest that a dual-response to multispecies by a single TP fluorescent probe must be more appropriate for imaging the redox process and offer crucial information for biomedical research.

Herein, we designed and synthesized a single mitochondria-targeting ratiometric fluorescence probe (4-((6-(2,2-dicyanovinyl) naphthalene-2-yl)oxy)butyl)triphenyl phosphonium (DNB) for the redox homeostasis process between SO_2 and HClO in cells and in vivo. The synergistic detection of SO_2 and HClO were achieved via a versatile malononitrile receptor (Scheme1). The selectively recognition of SO_2 and HClO through nucleophilic addition and oxidation reaction regulated the electron-donating ability of the probe DNB and resulted in intramolecular charge transfer (ICT)-induced distinct blue shifts in the emission spectrum. Then the ratiometric fluorescence signals occurred. DNB exhibited fast response time to SO_2 (< 50 s) with a blue-shift of 175 nm in fluorescence emission. The response time to HClO was within 20 s coupled with a 75 nm blue-shift. As a mitochondria-targeting fluorescence probe, DNB was successfully applied to detect endogenous SO_2/HClO in cells and image redox cycle between SO_2 and HClO in zebrafish.

Experimental Section

Materials and instruments used in this work, preparation of various ROS, RSS and RNS, absorption and fluorescent analysis, quantum yield calculation, detection of limits and the measurement of two-photon cross section are given in supporting information.

Synthesis of (4-((6-formylnaphthalen-2-yl)-oxy) butyl) triphenylphosphonium (BTP): A solution of 6-Hydroxy-2-naphthaldehyde (172 mg, 1.0 mM) in anhydrous acetonitrile (20 ml) was trearted with K_2CO_3 (0.272 g, 2.0 mM), solution was stirred at 60 °C for 30 min, then, (4-bromobutyl)triphenylphosphonium bromide (478 mg, 1.0 mM) upon addition. The mixture was heated under reflux overnight, filtered and collected colature. Organic layer was separated and evaporated under reduced pressure. Purification by column chromatography on silica eluting with CH_2Cl_2 (25:1 v/v) gave a white solid 245 mg, yield 43%. LC-MS (ESI+): m/z $C_{33}H_{30}O_2P^+$ calcd. 489.20 found [M^+] 489.2. ^{1}H NMR (500MHz, DMSO-d^6) δ/ppm 10.07(s,1H), 8.48 (s, 1H), 8.06-8.04 (d, J=10 Hz, 1H), 7.92-7.90 (d, J=10 Hz, 1H), 7.86-7.78 (m, J=35 Hz, 7H), 7.71 (s, 1H), 7.55-7.51 (q, J=22Hz, 8H), 7.43-7.42 (d, J=5 Hz, 1H), 7.25-7.21(q, J=20 Hz, 1H), 4.16-4.13 (t, J=12.5 Hz, 2H) 2.50-2.43 (m, J=28.5 Hz, 2H), 1.93-1.89 (q, J=20 Hz, 2H), 1.66-1.64 (t, J=8.8 Hz, 2H). ^{13}C, NMR (125MHz, DMSO-d^6) δ/ppm 192.9, 159.6, 138.3, 134.8, 134.1, 132.4, 131.9, 131.7, 130.9, 130.8, 129.1, 129.0, 128.1, 123.4, 120.3, 107.6, 67.67, 29.90, 28.06, 18.47.

Synthesis of (4-((6-(2,2-dicyanovinyl) naphthalene-2-yl) oxy) butyl) triphenyl phosphonium (DNB): BTP (245 mg, 0.5 mM) was dissolve in 10 ml DMF, and 0.1 mL pyridine was added, and string at 60 °C for 30 min, then 0.132 g malononitrile was dropped and string for 10 h. After reaction completely, mixture was poured into 20 ml water, then CH_2Cl_2 (3× 20 ml) was used to extract and combined organic layer to get yellow raw yield. Further purified by column chromatography on silica eluting with CH_2Cl_2 (50:1 v/v) to get a light yellow solid, 90 mg, yield 65%. LC-MS (ESI+): m/z $C_{36}H_{30}N_2OP^+$ calcd. 537.21 found [M+] 537.2. δ/ppm 10.07(s,1H), 8.57 (s, 1H), 8.39 (s, 1H), 8.06-8.04 (d, J=10 Hz, 1H), 7.97-7.94 (q, J=15 Hz, 2H), 7.81-7.77 (m, J=20 Hz, 6H), 7.55-7.50 (q, J=25Hz, 9H), 7.43-7.42 (d, J=5 Hz, 1H), 7.24-7.22 (q, J=10 Hz, 1H), 4.17-4.14 (t, J=15 Hz, 2H) 2.50-2.45 (q, J= 25 Hz, 2H), 1.92-1.88 (q, J=20 Hz, 2H), 1.66-1.63 (q, J=15 Hz, 2H). 13C, NMR (125MHz, DMSO-d6) δ/ppm 161.64, 160.27, 137.85, 135.23, 134.84, 134.08, 131.96, 130.93, 130.85, 129.15, 129.06, 128.46, 127.86, 124.89, 120.89, 101.78, 67.82, 49.05, 29.73, 28.02, 18.42.

Cell Culture: HeLa cells and Raw 264.7 cells were purchased from the Committee on Type Culture Collection of Chinese Academy of Sciences (Shanghai, China). HeLa cells were incubated in DMEM (Dulbecco's Modified Eagle Medium) supplemented with 10% fetal bovine serum (FBS). Raw 264.7 cells were incubated in RPMI (Roswell Park Memorial Institute) 1640 Medium supplemented with 10% (FBS) at 37 °C under a humidified atmosphere containing 5% CO2. The cells were passaged by scraping and seeding on 20 mm Petri-dishes according to the instructions from the manufacturer.

Cell imaging: Florescent images were acquired on Carl Zeiss LSM880 with a multiphoton laser scanning microscope with an objective lens (× 40) and set excitation wavelength at 700, 760 and 850 nm, respectively. Cells were plated on Petri-dishes (Φ = 20 mm)

View Article Online
DOI: 10.1039/C7TB01900A

and allowed to adhere for 24 hours before imaging. The probe was added to the culture plates which were filled with 1.5 mL fresh complete medium. Prior to imaging, the medium was removed. Cell imaging was carried out after washing cells with cultured medium for three times to remove the excess adding compounds.

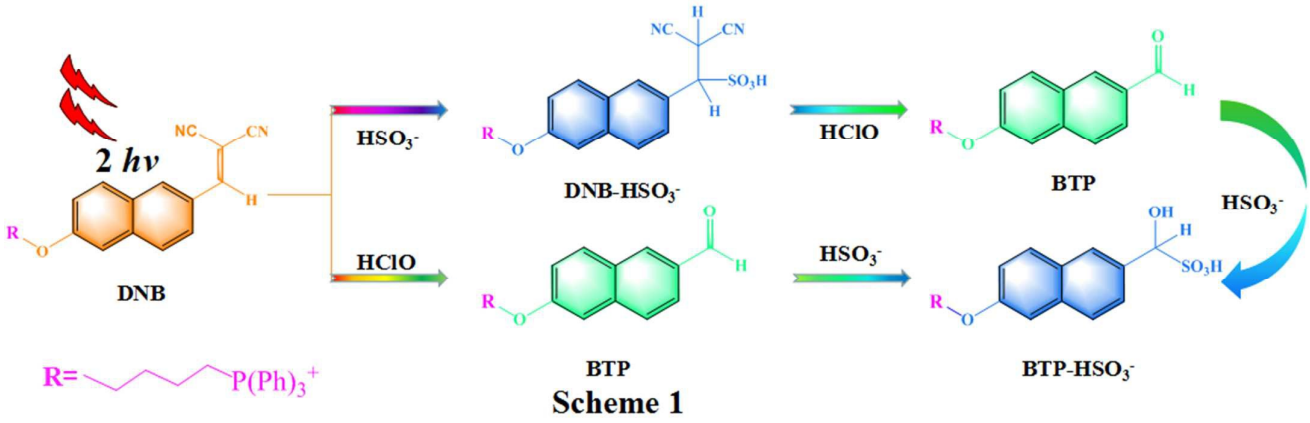

Scheme 1

Scheme 1. Illustration for the structure of DNB and its response mechanism

Fluorescence imaging in zebrafish: Zebrafish were purchased from the Huan Te biological corporation (Hangzhou, China). For imaging endogenous HSO3- zebrafish larvae (three-days) were put into a 50 mm Petri dish filled with E3 media (15 mM NaCl, 0.5 mM KCl, 1mM MgSO4, 1 mM CaCl2, 0.15 mM KH2PO4, 0.05 mM Na2HPO4 and 0.7 mM NaHCO3; pH 7.50) containing SO2 donor, then 2.0 μM probe added and incubated for one hour, then, E3 media was used to remove the residual probe. Subsequence, for imaging endogenous HClO, zrbrafish were pretreat LPS and PMA (1μg/mL) were incubated for different times, then 2.0 μM probe added and further incubated for one hour. TP fluorescence microscopy images were carried out with a mode-locked titanium-sapphire laser source set excitation wavelength at 700, 760 and 850 nm, respectively.

Results and discussion

Design and synthesis of probe DNB

To achieve the synergistic detection of SO_2/HClO during redox homeostasis process in cells and in vivo, we have to comprehend chemical properties of SO_2 and HClO. SO_2 will rapidly hydrate to bisulfite (HSO_3^-) and sulfite (SO_3^{2-}). These derivatives selectively exhibit strong nucleophilic abilities to aldehydes/ketones and poor-electronic double bonds.[40] In this work, HSO_3^- is used as the representative form of SO_2 in solution. HClO is a weak acid with a pKa of 7.53, which cannot be isolated from aqueous solution. HClO contributes to bioeffects in cells via its oxidation capacity to a wide variety of biomolecules including unsaturated fatty acid. After having checked the whole properties of SO_2 and HClO, we consider to preferentially introduce an unsaturated double bond into a fluorophore for the synergistic detection of SO_2/HClO.[41] The focus is on that the electron density of the selected double bond not only meets the nucleophilic addition of SO_2 but also suffices the oxidation reaction of HClO. All the reactions will result in changes in typical "push−pull" electronic effect of the probe and lead to spectral shifts in terms of the fluorescence emission. 6-Hydroxy-2-naphthaldehyde is chosen as the two-photo fluorophore due to its excellent photophysical properties.[42, 43] As shown in Scheme S1, the dual-response reaction unsaturated C=C receptor was obtained from Knoevenagel condensation reaction. Once linked the mitochondrial accumulation moiety (triphenylphosphonium cation), our probe DNB yielded. The potential processes for the synergistic detection of SO_2/HClO were illustrated in Scheme 1. HSO_3^- easily conjugated the unsaturated double bond nucleophilic addition reaction benefitting from the electron-withdrawing malononitrile moiety. Adduct could be next oxidized to the original aldehyde TP fluorophore (BTP) by HClO. The corresponding aldehyde group also could be utilized to further detect HSO_3^-. If the double bond was firstly oxidized by HClO, the reaction product was still the original aldehyde TP fluorophore (BTP) which could detect HSO_3^- in cells. To our delight, each detection process has its own unique spectral changes (Scheme 1 and Fig. 1), which completely met the requirement of the synergistic detection of SO_2/HClO in cells and in vivo. MS-APCI was employed to verify the reaction mechanism in scheme 1. The collision-induced dissociation spectra of the adduct of DNB-HSO_3^- produced a specific fragment ion $[DNB+HSO_3^-+H]^+$ at m/z 619.1 (Fig. S2a). A fragment ion at m/z 489.2 was found from the cleavage of C=C double bond via the oxidation mechanism of HClO (Fig. S2b). ^{1}H NMR spectroscopy was used to further confirm the mechanism. As shown in Fig. S3 and Fig. S11, DNB exhibit a peak of olefin at δ=8.57 ppm (H_1), once added HSO_3^-, two new peaks were observed at δ=4.50 ppm (H_2) and δ= 3.18 ppm (H_1), respectively. It was obvious that the addition reaction occurred on the C=C double bond. ^{1}H NMR spectra of DNB gave an alkene proton signal at δ=8.57 ppm. When added HClO, the alkjene proton signal disappeared and a new signal peak at δ= 10.08 ppm emerged.

Spectral properties of DNB toward HSO_3^- and HClO

We investigated the ability of DNB toward HSO_3^- in PBS buffer solution (pH 7.4, 20 mM, containing 10% DMSO v/v). As shown in Fig. S4a, the probe DNB (2 μM) exhibited an absorption peak at 425

View Article Online
DOI: 10.1039/C7TB01900A

nm. Once added HSO_3^-, a blue-shift absorption peak at 350 nm was observed. The isosbestic point was at 385 nm. For the fluorescence spectra, the addition of HSO_3^- remarkably decreased the emission peak at 600 nm and simultaneously emerged an obvious blue-shifted peak at 425 nm (Fig. 1a, 1b). The peak continuously increased until the final concentration of HSO_3^- was at 25 μM. In the detection process, the colour of the solution was changed from red to blue. The

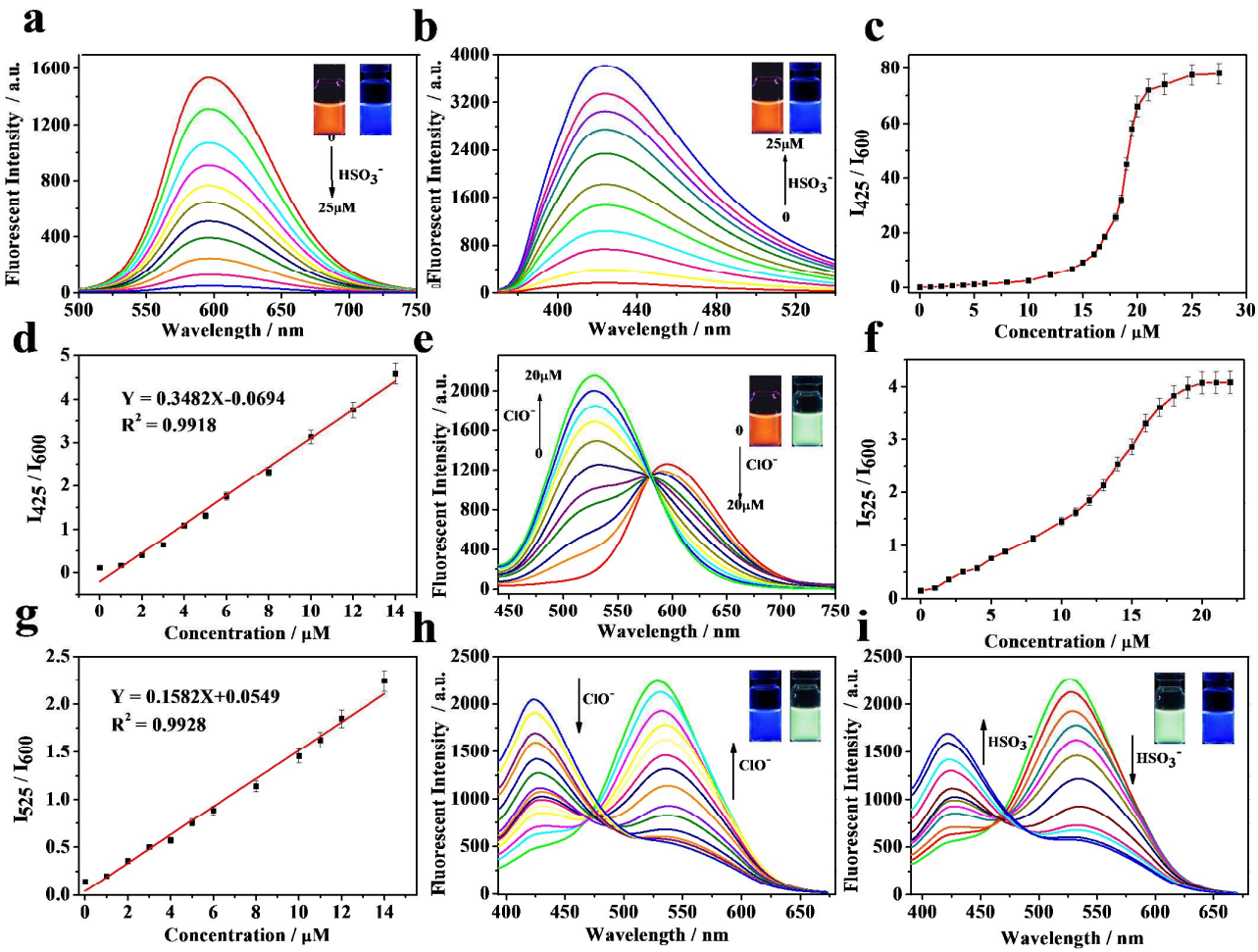

Fig. 1 Fluorescence response of probe DNB (2 μM) to HSO_3^- and HClO were respectively investigated in PBS buffer solution (10% DMSO v/v, pH = 7.4, 20 mM). a): Fluorescence response at 600 nm (λex = 460 nm) to HSO_3^- (0 to 25 μM); b): Fluorescence response at 425 nm (λex = 350 nm) to HSO_3^- (0 to 25 μM); c): The plot of fluorescence ratios (I425 nm/I600 nm) versus the concentrations of HSO_3^-; d) The linear curve established by fluorescence ratios ($I_{425\ nm}/I_{600\ nm}$) versus the concentrations of HSO3-; e): The fluorescence response (λex = 420 nm) of DNB (2 μM) to HClO (0 to 20 μM); f): The plot of fluorescence ratios ($I_{525\ nm}/I_{600\ nm}$) versus the concentrations of HClO; g): The linear curve established by fluorescence ratios ($I_{525\ nm}/I_{600\ nm}$) versus the concentrations of HClO; h): The fluorescence response of the DNB-HSO_3^- (see Scheme 1) to increased HClO (0-50 μM) (λex = 380 nm). i): The fluorescence response of the BTP (Scheme 1) to increased HSO_3^- (0-50 μM) (λex = 380 nm).

quantum yield of the DNB-HSO_3^- (Φ = 0.56) is about 2.5-fold higher than that of DNB. The maximum TP action cross-section (Φδ) were determined to be 52 GM and 73 GM at 850 and 700 nm, respectively. The intensity ratios at the two emission wavelengths ($I_{425\ nm}/I_{600\ nm}$) had a good linear (r = 0.9956) at the given concentration range of 0 - 14 μM HSO_3^-. The limit of detection was calculated to be as low as 8.0 nM (3σ/k). We next illustrated the ability of DNB to detect HClO. When added HClO (the source was NaClO), a new absorption peak at 380 nm emerged. The isosbestic point was at 405 nm (Fig. S4b). With excited by the light at 420 nm, the corresponding fluorescence spectral changes of DNB were shown in Fig. 1e. With the increasing amount of HClO was added into the solution of DNB, a fluorescence emission peak increased with a center at 525 nm. The fluorescence intensity kept constant when over 10 eq. HClO was added. Quantum yield of the oxidized DNB was determined to be 0.45. The TP action cross-section (Φδ) were determined to be 69 GM at 760 nm. A 4.1-fold fluorescence ratio was obtained ($I_{525\ nm}/I_{600\ nm}$) following a color change from red to green. There was a good linear relationship between fluorescence ratio and the concentration of HClO ranging from 0 to 14 μM (r = 0.9964). The calculated limit of detection was 15.2 nM. We further inspect whether DNB-HSO_3^- could be used to successively react with HClO. As shown in Fig. 1h, the fluorescence peak of DNB-HSO_3^- (425 nm) gradually decreased with the addition of HClO, and an emission peak at 525 nm arose. The corresponding MS and NMR spectroscopy were used to confirm the reaction (Fig. S2 and S3). We then checked whether the oxidation product could be used to response to HSO_3^- again. As expected, after added an excessive amount of HSO_3^-, there emerged a new fluorescence peak at 420 nm (Fig. 1i). These results potentially demonstrated that our probe DNB

View Article Online
DOI: 10.1039/C7TB01900A

not only could detect HSO_3^- and HClO, respectively, but also could applied to indicate HClO induced oxidative stress in the presence with antioxidant capacity of SO_2. We wanted our probe could track the metabolic process of HSO_3^- in organism against oxidative stress caused by HClO.

Time dependent response and pH effects

The time response of our probe DNB (2.0 μM) towards HSO3- were tested. The fluorescence emission of DNB exhibited a smooth and steady signal level in the absence of HSO3-. However, the signal immediately decreased to a plateau within 50 s upon the addition of 15 μM HSO_3^- (Fig. S5a). The time response to HClO was also evaluated. With the addition of 15 μM HClO to the solution of 2 μM DNB, the fluorescence signal reached a plateau within 20 s (Fig. S5b). All the data indicated that DNB had fast dual-response to the detection of HSO_3^- and HClO via ratiometric fluorescence emission. The pH effects on fluorescence ratios of DNB for HSO_3^- and HClO were checked, respectively. As shown in Fig. S6, pH had almost no effects on the fluorescence emission of DNB in the range of pH 4.0-10.0. Upon the addition of 15 μM HSO_3^-, the fluorescence ratio ($I_{425\ nm}/I_{600\ nm}$) increased with the increased pH from 6.0 to 10.0. The results indicated that the nucleophilic addition reaction between DNB and HSO_3^- was favorable in neutral. The pH was also compatible with the pKa of HSO_3^- (pKa=7.20). The effect of pH on the fluorescence ratio of DNB to HClO was also evaluated. With the addition of HClO, the fluorescence ratio ($I_{525\ nm}/I_{600\ nm}$) was increased with the increased of pH value. The ratio was obviously appropriate when pH was set at 7.4. The results indicated that our probe DNB could well function under physiological conditions.

Selectivity

To evaluate the selectivity of DNB to HSO_3^-/HClO, the interferences coming from various biologically relevant species were examined. The anions included Cl^-, Br^-, I^-, CH_3COO^-, ClO_4^-, SO_4^{2-}, $H_2PO_4^-$, $S_2O_3^{2-}$, and SCN^-. RSS contained HS^-, GSH, Cys, and Hcy. Reactive oxygen/nitrogen species (ROS/RNS) involved H_2O_2, ·OH, TBHP, TBO^-, KO_2, $ONOO^-$, NO_2^-, NO_3^-, and NO. Fluorescence intensity ratio ($I_{425\ nm}/I_{600\ nm}$) of the probe upon the addition of interferences were recorded in (Fig. 2a), it was clear that DNB showed a negligible response to anions and RSS compared with HSO_3^-. Moreover, even the 15-fold excess of HS- did not affect the detection of HSO_3^-. DNB exhibited a high selective ability towards HSO_3^- and

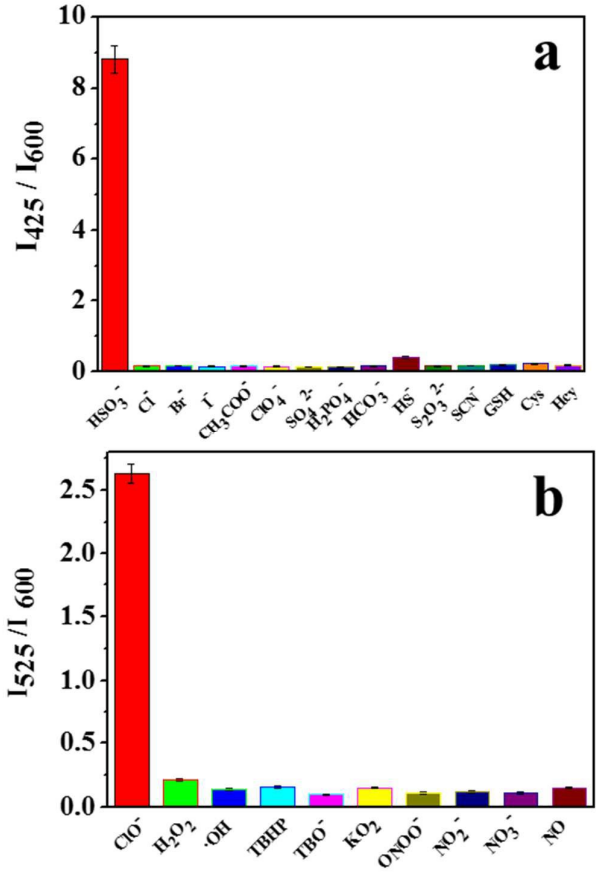

Fig. 2 a) Fluorescence ratio response of DNB (2 μM) towards HSO_3^- (15 μM) and various species: anions (1 mM), HS^-, $S_2O_3^{2-}$ (0.25 mM) and other biological thiols (0.5 mM). b) Fluorescence ratio response of DNB (2 μM) in the presence of HClO (15 μM) and various ROS and RNS (200 μM). All selective experiments were carried out in DMSO/PBS buffer solution (10/90, v/v, pH = 7.4, 20 mM).

View Article Online
DOI: 10.1039/C7TB01900A

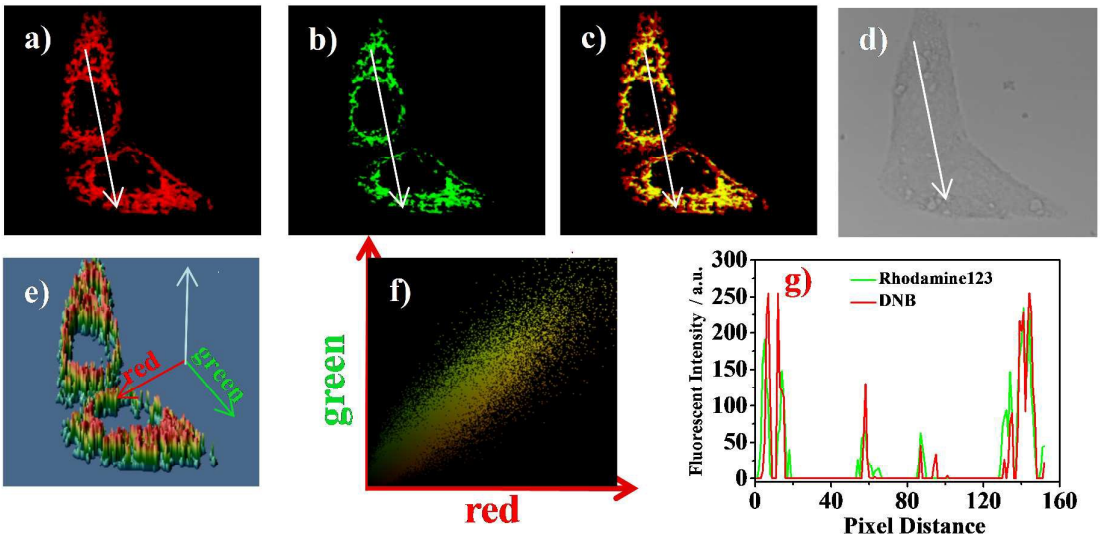

Fig. 3 Mitochondrial multicolor colocalization in HeLa cells with DNB and Rhodamine 123. Confocal fluorescence images of HeLa cells stained with a): 1 μM DNB and b) Rhodamine 123 (1 μg/mL) at 37 °C for 30 min; c): Merged image of a) and b); d): Bright field image; e): Perspective observation; f): Correlation plot of Rhodamine 123 and DNB intensities; g): Intensity profile of regions of interest (ROI) across HeLa cells. Fluorescence confocal microscopic images constructed from 560 to 660 nm for a) λ_{ex} = 850 nm, from 500 to 570 nm for b) λ_{ex} = 488 nm, respectively. Scale bar: 10 μm.

provided an accurate method for the detection of HSO_3^- in complex physiological environments. The evaluation for the interferences coming from ROS and RNS were investigated. As shown in (Fig. 2b), no obvious fluorescence changes (ratios $I_{525\ nm}/I_{600\ nm}$) were observed in the presence of various ROS and RNS, which indicated that DNB showed excellent selectivity toward HClO excluding other ROS and RNS.

Mitochondrial localization

Before cell imaging, MTT assays were performed to reveal that the cell viability (Fig. S8). Even incubated with 20 μM DNB for 24 h, the cells still remained more than 90% good morphology. The results displayed that the cytotoxicity of DNB was very low, and it was suitable for living cell imaging. Mitochondria are known as the main organelles for the source of ROS and RSS. The subcellular detection of HSO_3^- and HClO in mitochondrial could provide significant information when defined their biological roles. We then examined the subcellular localization ability of DNB to mitochondria. The colocalization experiments were explored with a well-known mitochondrial staining dye Rhodamine 123. The fluorescent image of DNB and Rhodamin 123 was highly consistent with each other (Fig. 3). The Pearson's co-localization coefficient was employed to describe the correlation of dyes distribution between the two channels. The value was determined to be 0.958 in HeLa cells. The results demonstrated that the probe DNB displayed low cytotoxicity and desirable localization capacity to image in livi ng cells.

Imaging and quantification of endogenous SO_2

The potential applications for the imaging and quantification of intracellular HSO_3^-/HClO were investigated. The ability of DNB for the detection of HSO_3^- in cells was shown in Fig. 4. As control, HeLa cells were treated with formaldehyde to eliminate HSO_3^-.[44] After incubated with DNB (2 μM) at 37 °C for 30 min, HeLa cells exhibited strong red fluorescence (Fig. 4a). By contrast, if the cells were treated with various concentrations of HSO_3^- (0 μM, 5 μM, 10 μM, 20 μM, and 30 μM) at 37 °C for 30 min, the fluorescence of the red channel gradually decreased and the fluorescence of the blue channel turned on with the increasing of HSO_3^- concentrations (Fig. 4b-f). The results suggested that our probe DNB was able to detect the changes of HSO_3^- concentrations in cells. We next carried out assay to determine endogenous HSO_3^-. N-benzyl-2,4-dinitrophenylsul fonamide (synthesis in Scheme S2) could release SO_2 (HSO_3^-) in cells with the reaction of intracellular thiols (Fig. S9).[41] To investigate the generation of endogenous SO_2 via ratiometric fluorescence imaging, HeLa cells were pre-incubated with DNB probe (2 μM) at 37 °C for 30 min. There only observed red fluorescence with negligible blue fluorescence (Fig. 4b). When the pre-treated cells were incubated with SO_2 donor (20 μM) for another 30 min, the original red fluorescence from the red channel became weaker, and the blue fluorescence from HeLa cells became brighter (Fig. 4g). The ratio of I_{blue}/I_{red} also increased (Fig. 4i). If cells were first pre-incubated with 1.0 mM N-ethylmaleimide (NEM) for 30 min to deplete the intracellular thiols, there was no obvious fluorescence change in the red and blue channel (Fig. 4h). With the calibration curve, we evaluated the average level of endogenous HSO_3^- in cells. As shown in (Fig. 4i), the endogenous HSO_3^- derived from the SO_2 donor to be estimated at 5.2 ± 0.2 μM (standard deviation, n=11). The results demonstrated that the probe DNB could be applied to the qualitative and quantitative detection of intracellular HSO_3^-.

View Article Online
DOI: 10.1039/C7TB01900A

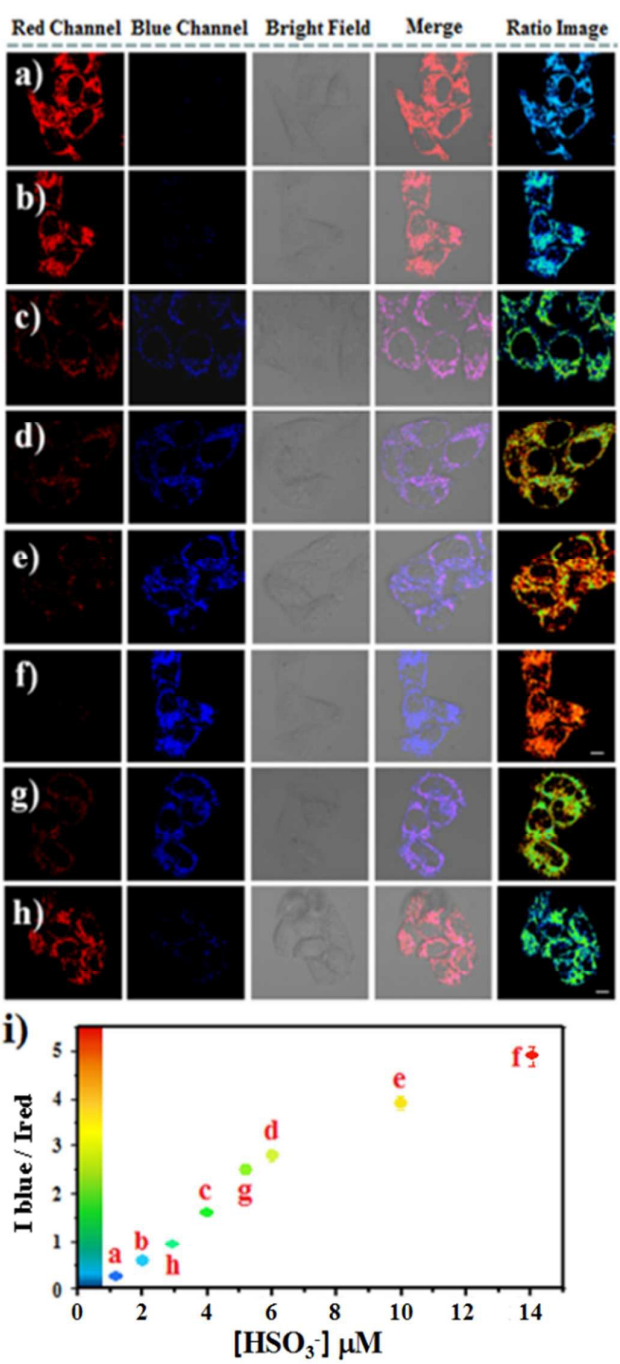

Fig. 4 a) – f) Two-photon microscopy images of HeLa cells with incubation of different levels of HSO_3^- for 30 min. a): 50 μM formaldehyde; b): 0 μM; c): 5 μM; d): 10 μM; e): 20 μM; f): 30 μM HSO_3^- were added into group b; g) –h) Two-photon fluorescence images of HeLa cells for endogenous HSO_3^-; g): The cells were incubated with N-benzyl-2,4-dinitrophenylsulfonamide (BTSA) for 30 min; h): After incubated with N-ethylmaleimide (NEM) (1 mM) for 30 min, the cells were treated as described in g); i) The average concentrations of HSO_3^- in HeLa cells calculated via fluorescence ratios of images a) – h). Error bars are ± SD, n=11. All the cells were pretreated with DNB (2 μM) for 30 min. TPM image was acquired by using 850 nm and 700 nm excitation and fluorescent emission windows at 560–660 nm and 420–470 nm, respectively. Scale bar: 10 μm.

Imaging and quantification of endogenous HClO

The excessive production of HClO could lead to cell damage. We next quantified the endogenous HClO in mouse macrophages (Raw 264.7 cells). The fluorescence ratio images of HClO in living cells were shown in Fig. 5. The cells in Fig. 5a were treated with taurine to eliminate the endogenous HClO.[45] When Raw 264.7 cells were incubated with the probe DNB (2 μM) for 30 min, we obtained a strong fluorescence in the red channel, but there was almost no fluorescence in the green channel. Followed by the incubation of concentrations of HClO (0 μM, 5 μM, 10 μM, 15 μM, 25 μM) for 30 min, the intracellular images of fluorescence in green channel increased and the corresponding red channel gradually decreased (Fig. 5b-f). The results demonstrated that DNB could evaluate the changes of HClO level in cells. Once stimulated with lipopolysaccharide (LPS) and phorbol myristate acetate (PMA), macrophages will endogenously produce HClO.[31] The detection of endogenous HClO was performed as follows: Raw 264.7 cells were incubated with DNB probe (2 μM) at 37 °C for 30 min. Subsequently, the cells were stimulated with LPS (1 μg/mL) and PMA (1 μg/mL) for 1h, there observed a strong fluorescence in the green channel and a weak fluorescence in the red channel (Fig. 5g). This high fluorescence ratio (I_{green}/I_{red}) was attributed to the reaction of our probe with HClO. To further elaborate the ability of our probe to detect endogenous HClO, one more experiment was carried out. 4-Aminobenzoic acid hydrazide (4-ABAH) could be used to reduce the intracellular level of HClO through inhibiting the activity of MPO. The cells in Fig. 5h were pretreated with 4-ABAH (50 μM) for 30 min. After washed by PBS buffer, the cells were treated as described in Fig. 5g. The green fluorescence was suppressed with a low fluorescence ratio of Igreen/Ired, which should be attributed to the reduced concentration of intracellular HClO because of the inhibitive effect of 4-ABAH for MPO.[46] With the calibration curve, the levels of HClO in cells were evaluated. As shown in Fig. 4i, the cells were stimulate by LPS and PMA gave a concentration of HClO at 4.8 ± 0.2 μM (SD, n = 11). We confirmed that our probe DNB was capable of quantifying endogenous HClO in cells.

Synergistic imaging SO_2/HClO crosstalk in vivo

When the overproduction of ROS lead to intracellular oxidative stress, the anti-oxidative and repair mechanisms of living organisms start to protect essential components of cells against the ROS damage. As known, Cys dioxygenase can catalyze Cys to cysteinesulfinate which further enzymatically converts to β-sulfinylpyruvate by aspartate aminotransferase, and finally decomposes to pyruvate and SO_2. Additionally, SO2 could be also endogenously produced via the oxidation of intracellular sulfur-containing amino acids by ROS.

We now strived to test the abilities of our TP probe DNB for the synergistic imaging SO2/HClO crosstalk in the physiological process of oxidative stress and anti-oxidative. Zebrafish has around 87% homologous genes with human, which is selected as animal mode. We firstly evaluated the level changes of HSO3-/HClO when the organism suffered from pathological oxidative stress. As shown in Fig. 6Aa, zebrafish incubated with DNB (2 μM) exhibited strong red fluorescence and almost no green and blue fluorescence. Then zebrafish were treated with BTSA (30 μM) for 30 min and 2 h, respectively (Fig. 6Ab-c). The fluorescence intensity in red channel

View Article Online
DOI: 10.1039/C7TB01900A

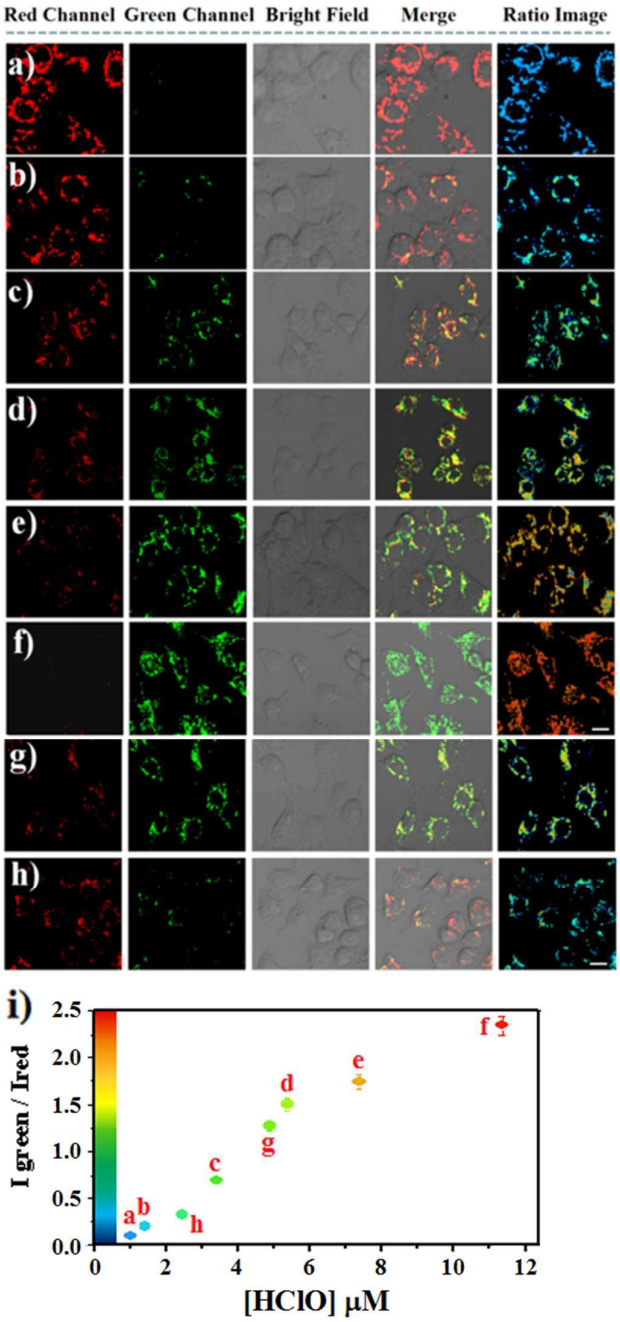

Fig. 5 a) – f) Two-photon microscopy images of Raw 264.7 cells with incubation of different levels of HClO for 30 min. a): 50 μM tuarine; b): 0 μM; c): 5 μM; d): 10 μM; e): 15 μM; f): 25 μM. g) –h) Two-photon fluorescence images of Raw 264.7 cells for endogenous HClO. g): The cells were incubated with LPS (1 μg/mL) and PMA (1 μg/mL) for 1 h; h): After incubated with 4-ABAH (50 μM) for 30 min, the cells were treated as described in g). i) The average concentrations of HClO in Raw 264.7 cells calculated via fluorescence ratios of images a) – h). Error bars are ± SD, n=11. All the cells were pretreated with DNB (2 μM) for 30 min. TPM image was acquired by using 850 nm and 760 nm excitation and fluorescent emission windows at 560–660 nm and 470–560 nm, respectively. Scale bar: 10 μm.

gradually decreased and the fluorescence intensity in blue channel gradually increased, which attribute to the release of SO_2 from BTSA. Once bacteria and pathogens invaded into living body, the defense system of the organism could made a fast response with a burst of HClO production. However, the overproduction of HClO could cause serious oxidative stress and cell apoptosis. The next experiment was

View Article Online
DOI: 10.1039/C7TB01900A

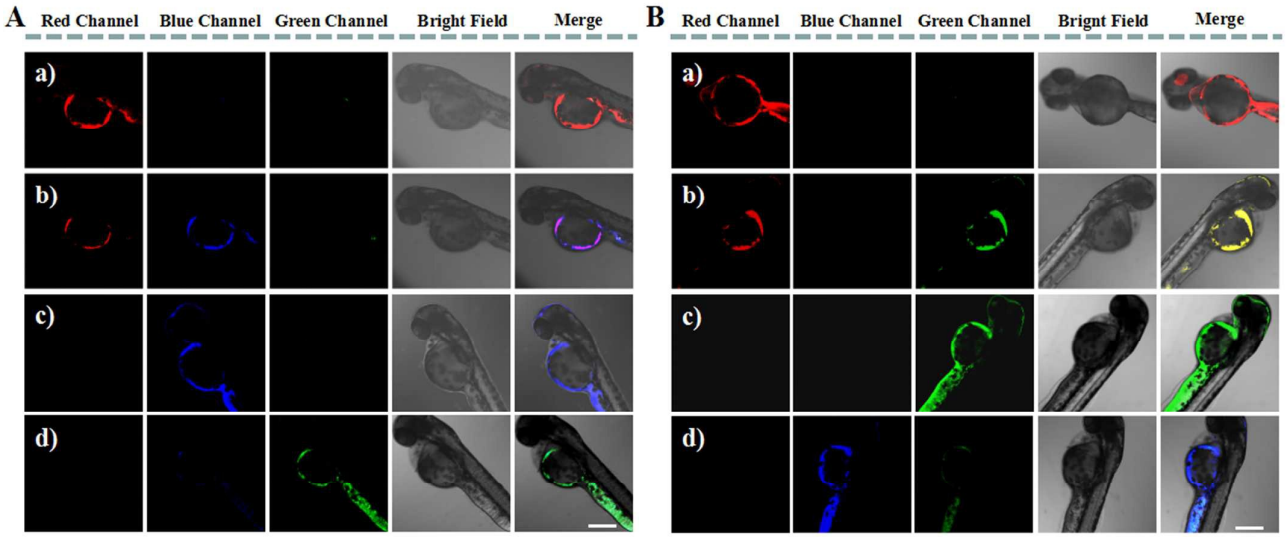

Fig. 6 A) TPM images of zebrafish for evaluating the successive changes between HClO and HSO_3^- under intracellular oxidative stress. Incubated with 2 μM DNB of 30 min a), then zebrafish were treated with BTSA (30 μM) for 30 min b) and 2 h c). d): After treated as described in c), LPS (2 μg/mL) and PMA (2 μg/mL) were added and further incubated for 3h. B) TPM images for investigating the levels of HClO/HSO_3^- under anti-oxidative metabolism of Cys. a): Treated as Figure 6Aa. b) and c): LPS (2 μg/mL) and PMA (2 μg/mL) were stimulated for 1h and 3h. d): After treated as described in c), added 500 μM Cys and further incubated for 2h. TPM image was acquired by using 850 nm, 700 nm and 760 nm excitation and fluorescent emission windows at 560 – 660 nm, 420 – 470 nm and 470 – 560 nm, respectively. TPM images were accumulated along the z direction with × 40 magnification at depths of 200 μm from the surface of zebrafish. Scale bar: 200 μm

carried out to further examine the process of oxidative stress that induced by abnormal HClO after the detection of SO_2. Zebrafish in Fig. 6Ac was further stimulated with LPS (2 μg/mL) and PMA (2 μg/mL) for 3h to in situ generate abundant HClO. As shown in Fig. 6Ad, an obvious fluorescence increase in green channel and the corresponding fluorescence intensity in blue channel became faint. The results indicated that the excessive HClO could consume anti-oxidative SO_2. Our probe exhibited excellent capability of the synergistic detection of HSO_3^-/HClO in vivo. We then explored the zebrafish model of anti-oxidative process and visualized the metabolism of Cys in the presence of HClO. Zebrafish were incubated by probe just exhibited negligible fluorescence in green and blue channels (Fig. 6Ba). Upon addition of LPS (2 μg/mL) and PMA (2 μg/mL), the blue emission began increased gradually in the next 3h (Fig. 6Bb-c). The results demonstrated the excessive generation of HClO in living body. To confirm our probe DNB could detect the metabolism of Cys, 500 μM Cys was added and then continuously incubated for another 2 h. As illustrated in Fig. 6Bd, the fluorescence response in green channel decreased and that of in blue channel increased. The reason was attributed to that Cys played an antioxidant role in eliminating the excessive HClO in vivo. However, SO_2, as the metabolite of Cys, could be successive captured by the HClO-oxidized probe and emitted strong blue fluorescence. These results confirmed that our probe DNB could achieve to the synergistic discrimination and detection of HSO3-/HClO in complex physiological milieu. These results also made DNB an appropriate tool for further exploring the relationship between HSO_3^- and HClO in cells and in vivo.

Conclusions

In summary, we develop a two-photon ratiometric fluorescent probe DNB for the synergistic detection of mitochondrial SO_2/HClO crosstalk in cells and in vivo. The probe offers large TP action cross-sections, low cytotoxicity, excellent selectivity, and high sensitivity for the synergistic detection of SO_2/HClO in cells and in vivo. This probe can be successfully used for real-time and imaging of the mitochondrial SO_2/HClO successive changes in HeLa and Raw 264.7 cells. This new probe also can estimate SO_2/HClO crosstalk at 200 μm depth in zebrafish employing two-photon microscopy. These results demonstrate that this probe potentially reveal.

Acknowledgements

This work was supported by the National Natural Science Foundation of China (Nos: 21475074, 21403123, 21375075, 31301595, 21402106, 21475075, 21275089, 21405093, 21405094, 81303179, 21305076), and the Funds of Shandong Province Key Laboratory of Detection Technology for Tumour Markers (KLDTTM2015-6, KLDTTM2015-9).

References

1 C. E. Paulsen and K. S. Carroll, *Chem. Rev.*, 2013, **113**, 4633-4679.
2 X. Chen, X. Tian, I. Shin and J. Yoon, *Chem. Soc. Rev.*, 2011, **40**, 4783-4804.
3 Y. Yue, F. Huo, P. Ning, Y. Zhang, J. Chao, X. Meng and C. Yin, *J. Am. Chem. Soc.*, 2017, **139**, 3181-3185.
4 L. Luo, S. Chen, H. Jin, C. Tang and J. Du, *Biochem. Bioph. Res. Co.*, 2011, **415**, 61-67.
5 W. Li, C. Tang, H. Jin and J. Du, *Atherosclerosis*, 2011, **215**, 323-330.
6 J. Li and Z. Meng, *Nitric Oxide*, 2009, **20**, 166-174.
7 Q. Zhang and Z. Meng, *Eur. J. Pharmacol.*, 2009, **602**, 117-123.

View Article Online
DOI: 10.1039/C7TB01900A

8 J. L. Wallace and R. Wang, *Nat. Rev. Drug. Discov.*, 2015, **14**, 329-345.
9 F. Yu, P. Song, P. Li, B. Wang and K. Han, *Chem. Commun.*, 2012, **48**, 7735-7737.
10 Y. Huang, F. Yu, J. Wang and L. Chen, *Anal. Chem.*, 2016, **88**, 4122-4129.
11 Q. Xu, K.-A. Lee, S. Lee, K. M. Lee, W.-J. Lee and J. Yoon, *J. Am. Chem. Soc.,* 2013, **135**, 9944-9949.
12 J. J. Hu, N.-K. Wong, M.-Y. Lu, X. Chen, S. Ye, A. Q. Zhao, P. Gao, R. Yi-Tsun Kao, J. Shen and D. Yang, *Chem. Sci.*, 2016, **7**, 2094-2099.
13 N. Branzk, A. Lubojemska, S. E. Hardison, Q. Wang, M. G. Gutierrez, G. D. Brown and V. Papayannopoulos, *Nat. Immunol.*, 2014, **15**, 1017-1025.
14 M. Valko, C. J. Rhodes, J. Moncol, M. Izakovic and M. Mazur, *Chem-Bio. Interact.*, 2006, **160**, 1-40.
15 D.-K. Choi, S. Pennathur, C. Perier, K. Tieu, P. Teismann, D.-C. Wu, V. Jackson-Lewis, M. Vila, J.-P. Vonsattel, J. W. Heinecke and S. Przedborski, *J. Neurosci.*, 2005, **25**, 6594-6600.
16 P. Nagy, K. Lemma and M. T. Ashby, *J. Org. Chem.*, 2007, **72**, 8838-8846.
17 M. Gao, F. Yu, H. Chen and L. Chen, *Anal. Chem.*, 2015, **87**, 3631-3638.
18 L. Yuan, L. Wang, B. K. Agrawalla, S.-J. Park, H. Zhu, B. Sivaraman, J. Peng, Q.-H. Xu and Y.-T. Chang, *J. Am. Chem. Soc.*, 2015, **137**, 5930-5938.
19 W. Xu, C. L. Teoh, J. Peng, D. Su, L. Yuan and Y. Chang, *Biomaterials*, 2015, **56**, 1-9.
20 F. Yu, M. Gao, M. Li and L. Chen, *Biomaterials*, 2015, **63**, 93-101.
21 F. Yu, P. Li, B. Wang and K. Han, *J. Am. Chem. Soc.*, 2013, **135**, 7674-7680.
22 X. Shen, E. A. Peter, S. Bir, R. Wang and C. G. Kevil, *Free. Radical. Bio. Med.*, 2012, **52**, 2276-2283.
23 A. Isaac, J. Davis, C. Livingstone, A. J. Wain and R. G. Compton, TrAC-Trends. *Anal. Chem.*, 2006, **25**, 589-598.
24 M. Koch, R. Köppen, D. Siegel, A. Witt and I. Nehls, *J. Agr. Food. Chem.*, 2010, **58**, 9463-9467.
25 Y. Zhang, L. Guan, H. Yu, Y. Yan, L. Du, Y. Liu, M. Sun, D. Huang and S. Wang, *Anal. Chem.*, 2016, **88**, 4426-4431.
26 W. Chen, Q. Fang, D. Yang, H. Zhang, X. Song and J. Foley, *Anal. Chem.*, 2015, **87**, 609-616.
27 Y. Wu, J. Wang, F. Zeng, S. Huang, J. Huang, H. Xie, C. Yu and S. Wu, *ACS Appl. Mater. Interfaces.*, 2016, **8**, 1511-1519.
28 Q. A. Best, N. Sattenapally, D. J. Dyer, C. N. Scott and M. E. McCarroll, *J. Am. Chem. Soc*., 2013, **135**, 13365-13370.
29 H. Zhu, J. Fan, J. Wang, H. Mu and X. Peng, *J. Am. Chem. Soc.*, 2014, **136**, 12820-12823.
30 X. Zhu, L. Zhu, H.-w. Liu, X. Hu, R. Peng, J. Zhang, X. Zhang and W. Tan, *Anal. Chim. Acta.*, 2016, **937**, 136-142.
31 Q. Xu, C. H. Heo, J. A. Kim, H. S. Lee, Y. Hu, D. Kim, K. M. K. Swamy, G. Kim, S.-J. Nam, H. M. Kim and J. Yoon, *Anal. Chem.,* 2016, **88**, 6615-6620.
32 F. Yu, P. Li, P. Song, B. Wang, J. Zhao and K. Han, *Chem. Commun.,* 2012, **48**, 2852-2854.
33 Z. Lou, P. Li, Q. Pan and K. Han, *Chem. Commun.*, 2013, **49**, 2445-2447.
34 F. Liu, T. Wu, J. Cao, H. Zhang, M. Hu, S. Sun, F. Song, J. Fan, J. Wang and X. Peng, *Analyst*, 2013, **138**, 775-778.
35 H. M. Kim and B. R. Cho, Chem. Rev, 2015, **115**, 5014-5055.
36 C. S. Lim, S. K. Das, S. Y. Yang, E. S. Kim, H. J. Chun and B. R. Cho, *Anal. Chem.*, 2013, **85**, 9288-9295.
37 S. K. Bae, C. H. Heo, D. J. Choi, D. Sen, E.-H. Joe, B. R. Cho and H. M. Kim, *J. Am. Chem. Soc.,* 2013, **135**, 9915-9923.
38 J.-W. Choi, S. T. Hong, D. E. Kang, K. C. Paik, M. S. Han, C. S. Lim and B. R. Cho, *Anal. Chem.*, 2016, **88**, 9412-9418.
39 W. Kuo, C. Chang, H. Chen, C. L. Hsu, J. Wang, H. Kao, L. C. Chou, Y. Chen, S.-J. Chen, W.-T. Chang, S.-W. Tseng, P.-C. Wu and Y.-C. Pu, *ACS Appl. Mater. Interfaces*, 2016, **8**, 30467-30474.
40 F. Yu, X. Han and L. Chen, *Chem. Commun.*, 2014, **50**, 12234-12249.
41 K. Dou, Q. Fu, G. Chen, F. Yu, Y. Liu, Z. Cao, G. Li, X. Zhao, L. Xia, L. Chen, H. Wang and J. You, *Biomaterials*, 2017, **133**, 82-93.
42 S. Singha, Y. W. Jun, J. Bae and K. H. Ahn, *Anal. Chem*., 2017, **89**, 3724-3731.
43 L. He, X. Yang, Y. Liu, X. Kong and W. Lin, *Chem. Commun.,* 2016, **52**, 4029-4032.
44 Y. Tang, X. Kong, A. Xu, B. Dong and W. Lin, *Angew. Chem., Int. Edit.*, 2016, **55**, 3356-3359.
45 B. Wang, P. Li, F. Yu, P. Song, X. Sun, S. Yang, Z. Lou and K. Han, *Chem. Commun.*, 2013, **49**, 1014-1016.
46 M. Fujihara, M. Muroi, K.-i. Tanamoto, T. Suzuki, H. Azuma and H. Ikeda, *Pharmacol. Therapeut.*, 2003, **100**, 171-194

View Article Online
DOI: 10.1039/C7TB01900A

Table of contents entry

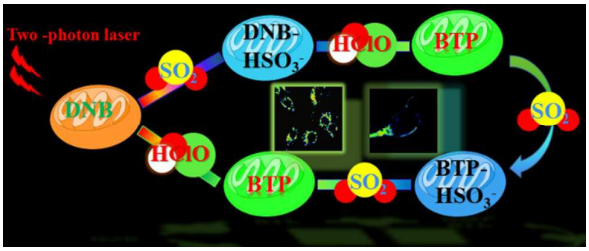

We reported a mitochondria-target two-photon ratiometric fluorescent probe to respectively or successively detect HSO_3^-/HClO in cells and zebrafish